Wave Friction Factors in Nearshore Sands

C. SMYTH AND ALEX E. HAY

Department of Oceanography, Dalhousie University, Halifax, Nova Scotia, Canada

(Manuscript received 2 January 2002, in final form 4 June 2002)

ABSTRACT

Wave friction factors are estimated from vertical profiles of near-bed turbulence and horizontal velocity spanning the wave bottom boundary layer. Measured values are partitioned by bed state, which ranged from irregular ripples to flat bed, and are examined as a function of two traditionally selected parameters—physical bed roughness and outer flow Reynolds number. The measurements are from two field experiments in very different nearshore environments: a relatively protected unbarred pocket beach and a linear barred beach exposed to the open shelf (Duck). Measured wave friction factors are remarkably similar for the two beaches and are highest for low-energy rippled beds and lowest for the high-energy flat bed conditions. The reduction in the friction factor for high-energy conditions corresponds to a decrease in the physical roughness of the bed as wave energy increases. As a function of relative roughness, measured friction factors are generally consistent with previous laboratory results and theoretical results for the high-energy cases, but the predicted values for the low-energy rippled beds show some significant differences. A new expression is derived for the bed roughness and is found to have a stronger dependence on ripple steepness than previously suggested laboratory-based relationships. Estimated friction factors exhibit a power-law dependence on Reynolds number and occupy a narrow band within the rough turbulent and transition regions.

1. Introduction

In shallow water, surface gravity wave energy is dissipated by bottom friction and frictional processes at the air–sea interface. For seabeds composed of noncohesive sandy sediments, the dissipation of wave energy in the bottom boundary layer is strongly dependent on the presence of sand ripples formed by the near-bed wave orbital motion. Bottom friction is important in sediment transport modeling (Nielsen 1992, p. 283), and several authors suggest that bottom friction is an important dissipation mechanism for energetic swell propagating across the continental shelf (Ardhuin et al. 2001; Young and Gorman 1995). In order to accurately predict wave heights, Tolman (1994) parameterized the interaction of waves with a mobile sandy bed using a laboratory-based ripple roughness predictor from Madsen et al. (1990) with a hydrodynamic model Grant and Madsen (1982) extended to spectral waves (Madsen et al. 1988). Within the sheet flow regime, Tolman (1994) used results by Wilson (1989) that were extrapolated to oscillatory boundary layers. However, Tolman (1994) and Nielsen (1992, p. 146) note that the available estimates of laboratory friction factors vary widely and that field estimates are sparse. In order to improve the accuracy of bottom friction estimates in natural conditions, in situ observations combining measurements of both the wave friction factor and bed state are needed.

In this study, wave friction factors are estimated over mobile sandy beds in the nearshore environment during storm and nonstorm conditions. This work builds on previous results by Smyth et al. (2002) and Smyth and Hay (2001, manuscript submitted to *J. Geophys. Res.*, hereafter SH) in which wave friction factors were estimated from turbulent velocities measured by an acoustic coherent Doppler profiler at two experiment sites in water depths of 3–4 m for a variety of wave conditions. It was found that peak average turbulence intensities were relatively independent of bed state, varying by no more than 50% despite a factor of 7–10 variation in average wave energy. This intriguing observation was explained by the corresponding decrease in the physical roughness of the bed, associated with active adjustment among different observed bedstates, as the wave energy increased. In the present study, additional wave friction factors estimates are obtained from the same data using the integrated acceleration defect equation, and are compared to our earlier turbulence-based estimates and to bottom friction estimates based on the Madsen et al. (1990) relationship. Their results apply over a small range of wave energies, and it is not clear if extrapolation over a wider range of wave energies is valid. This study will compare extrapolated values to the present measurements.

Corresponding author address: C. Smyth, Department of Oceanography, Dalhousie University, 1355 Oxford St., Halifax, NS B3H 4J1, Canada.
E-mail: csmyth@phys.ocean.dal.ca

The first objective is to place the measured wave friction factors within the context of previous results through comparison to theoretical, empirical, and model results. Predictive relationships for the wave friction factor are traditionally formulated in terms of two parameters—the bed roughness and the Reynolds number. Estimated friction factors may differ from laboratory results for fixed grain roughness that do not account for the added roughness contribution from mobile sediment grains (Grant and Madsen 1982; Nielsen 1992), and regular waves produce different bedform dimensions than irregular waves (Nielsen 1992, p. 136).

A second objective is to assess the importance of the mobile roughness contribution based on field measurements and fixed-roughness laboratory results. There is no generally accepted form for the bed roughness, and two formulas are used. The first is based on steady flow results (Grant and Madsen 1982), and the second on a compilation of previous oscillatory flow results (Wikramanayake and Madsen 1994).

The next section briefly describes previous theoretical and experimental wave friction factor results. A brief description of the data and methods is found in section 3, and measured friction factors are presented as a function of relative roughness in section 5 and of the Reynolds number in section 6. A new parameterization for the bed roughness is discussed in section 7, followed by the conclusions.

2. Theory and previous results

Jonsson (1966) defined the wave friction factor, f_w, in terms of the maximum bed shear stress τ_0 during a wave cycle,

$$f_w = \frac{2|\tau_0|}{\rho(A\omega)^2}, \tag{1}$$

where ρ is the fluid density, A is the near-bed wave semiexcursion distance, and ω is the wave angular frequency. The linearized equation of motion for flow in the wave boundary layer is given by

$$\rho\frac{\partial\tilde{u}_b}{\partial t} = -\frac{\partial p}{\partial x} + \frac{\partial\tau}{\partial z}, \tag{2}$$

where $\tilde{u}_b$ is the horizontal velocity, p is the pressure, τ is the shear stress, x is the horizontal coordinate (positive onshore), and z is the vertical coordinate (positive up). In the boundary layer approximation, the pressure gradient is assumed to be independent of z, giving

$$\rho\frac{\partial}{\partial t}(\tilde{u}_b - \tilde{u}) = \frac{\partial\tau}{\partial z}, \tag{3}$$

where $\tilde{u}$ is the free-stream velocity. The bottom stress is obtained by integrating the momentum equation across the boundary layer thickness δ:

$$\rho\int_{z_0}^{\delta+z_0}\frac{\partial}{\partial t}(\tilde{u}_b - \tilde{u})\,dz = -\tau(z_0), \tag{4}$$

where z_0 is the height at which the velocity goes to zero.

The friction factor may be derived theoretically through the velocity defect following Fredsoe and Deigaard (1992, p. 23). The velocity profile is assumed to be logarithmic:

$$\tilde{u}_b = \frac{u_*}{\kappa}\ln\left(\frac{z}{z_0}\right), \tag{5}$$

where u_* is the friction velocity and κ is von Kármán's constant. Solving for the wave friction factor gives an approximate form

$$f_w = 0.04\left(\frac{A}{k_N}\right)^{-1/4}, \qquad \frac{A}{k_N} > 50, \tag{6}$$

where k_N is the equivalent Nikuradse roughness ($k_N = 30z_0$), which agrees well with laboratory estimates by Kamphuis (1975) using a shear plate, estimates by Sleath (1987) using velocity defect relation with laser Doppler velocimeter measurements, and estimates by Jensen et al. (1989) using a flush-mounted hot film (Jensen et al. 1989). All three of these laboratory studies used fixed grain roughness.

Based on laboratory measurements, Jonsson (1966) obtained the friction factor in terms of the relative roughness, A/k_N, for fixed grain roughness:

$$\frac{1}{4\sqrt{f_w}} + \log_{10}\frac{1}{4\sqrt{f_w}} = -0.08 + \log_{10}\left(\frac{A}{k_N}\right). \tag{7}$$

A similar result was found in laboratory measurements, also for fixed grain roughness, by Kamphuis (1975):

$$\frac{1}{4\sqrt{f_w}} + \log_{10}\frac{1}{4\sqrt{f_w}} = -0.35 + \frac{4}{3}\log_{10}\left(\frac{A}{k_N}\right), \tag{8}$$

with an approximate form of

$$f_w = 0.4\left(\frac{A}{k_N}\right)^{-3/4}, \qquad \frac{A}{k_N} < 100 \tag{9}$$

for small A/k_N. Estimates of the friction factor using the Kamphuis (1975) result are generally smaller (50%–70%) than from the Jonsson (1966) formula, but typically there is considerable scatter in wave friction factor estimates (Nielsen 1992, p. 26).

Few measurements of friction factors exist for mobile beds and irregular waves. Madsen et al. (1990) estimated wave energy dissipation factors in the laboratory using irregular waves and mobile sediment. Their results showed

$$f_e = 0.29\left(\frac{\theta_d}{\theta_c}\right)^{-1.5}, \qquad 1.2 < \frac{\theta_d}{\theta_c} < 3, \tag{10}$$

where f_e is the wave dissipation factor, θ_d is the grain

roughness Shields parameter, and θ_c is the critical shear stress for initiation of grain motion. The wave energy dissipation factor relates the total energy available to the rate of energy dissipated by bed friction. Although the two friction coefficients f_w and f_e are defined differently, the experimental scatter is so large that they are often assumed to be equal (Nielsen 1992, p. 27).

Bed roughness formulations

Previous k_N parameterizations use length scales based on the sediment grain diameter and ripple height and/or ripple wavelength. For fixed grain roughness, the bed roughness was found to be proportional to grain size: $k_N = 2d_{50}$, Sleath (1987) and $k_N = 2d_{90}$, Kamphuis (1975), where d_{50} is the median grain diameter, and d_{90} is the 90th percentile grain diameter. For rippled beds, Sleath (1995) suggested that the bed roughness is proportional to ripple height, and Wikramanayake and Madsen (1994) found $k_N = 4\eta$ based on analysis of the limited data available for rippled beds. Grant and Madsen (1982) partitioned the bed roughness into ripple roughness, k_r, and moving grain roughness, k_s. They suggested that the ripple roughness is based on the physical roughness scale of the ripple,

$$k_r = 27.7\eta^2/\lambda, \tag{11}$$

where η is the ripple height and λ is the wavelength. Ripple roughness is characterized by the ripple height times the spatial concentration of the roughness elements, and the coefficient of 27.7 was derived using unidirectional flow data over 3D roughness arrays and assuming the law of the wall [Eq. (5)]. At low energies the ripple roughness dominates the total roughness, and the contribution from moving grain roughness increases with increasing wave energy.

For mobile beds and irregular waves, Madsen et al. (1990) estimated bed roughness using their measured wave friction factors and the boundary layer theory of Madsen et al. (1988):

$$\frac{A_{\text{rms}}}{k_N} = 0.67\left(\frac{\theta_d}{\theta_c}\right)^{2.5}, \tag{12}$$

where A_{rms} is the root-mean-square wave semiexcursion. This result is valid over a small range of measured wave energies, $1.2 < \theta_d/\theta_c < 3$, without reference to ripple type or dimension. In section 5, our measurements are compared to this equation over a wider range of wave energies.

3. Data summary

The first deployment was near Queensland Beach, Nova Scotia, in the fall of 1995 (hereafter referred to as QB95). Queensland Beach is a planar pocket beach *O*(100 m) long, located in a sheltered bay, and is oriented almost normal to wave energy entering the narrow mouth of St. Margaret's Bay from the open shelf (see Crawford and Hay 2001). In total, 11 days of data were collected in water depths of 3–4 m, depending on the tide. The sand had a median grain diameter of 175 μm. The second experiment was part of SandyDuck97 (hereafter SD97), which took place in the fall of 1997 near Duck, North Carolina. This experiment was located on a high-energy, linear barred beach in an open coast environment. There were 75 days of data collected in water depths of 3–4 m, and the sand had a median grain diameter of 170 μm.

TABLE 1. Field experiment parameters at the instrument location include deployment duration, significant wave orbital velocity $\tilde{u}_{1/3}$, ripple height η, and wavelength λ for the four bed states—irregular ripples (I), cross ripples (X), linear transition ripples (LT), and flat bed (F).

	I	X	LT	F
		QB95		
Data runs	63	77	14	14
$\tilde{u}_{1/3}$ (cm s^{-1})	25	34	51	68
η (cm)	0.9	2.3	0.33	
λ (cm)	17	72	10.7	
		SD97		
Data runs	77	43	19	16
$\tilde{u}_{1/3}$ (cm s^{-1})	32	45	58	82
η (cm)	0.72	1.78	0.45	
λ (cm)	18	75	8.9	

In both experiments, a 1.7-MHz coherent Doppler profiler (CDP) system measured an *O*(1 m) vertical profile of particle velocity and concentration with 0.7-cm vertical resolution Zedel and Hay (1999). For QB95, wave orbital velocities outside the wave boundary layer were measured at a height of 20 cm by a dual-beam CDP. Experiment parameters are given in Table 1. Longshore currents were not measured, but can reasonably be assumed to be small (Vincent et al. 1991). At SD97, wave orbital velocities were measured by an acoustic Doppler velocimeter (Sontek ADVO probe number 5036) at a height of 45–75 cm. Data runs included in this analysis had alongshore currents less than 20 cm s^{-1}. A thorough description of the experiments and the selected data runs is found in Smyth et al. (2002), SH, and Smyth (2001).

Bedform type was determined visually from rotary sonar images of the seafloor (A. E. Hay and T. D. Mudge 2002, unpublished manuscript). Bedform dimensions are shown in Fig. 1 as a function of mobility number ψ, where

$$\psi = \frac{\tilde{u}_{1/3}^2}{(s-1)gd_{50}}, \tag{13}$$

$\tilde{u}_{1/3}$ is the significant orbital velocity, s is the ratio of the particle to fluid density, d_{50} is the median sediment grain diameter, and g is acceleration due to gravity. Bedform dimensions, steepness, and bedform type were obtained using rotary fan-beam and pencil-beam sonars (Hay and Wilson 1994; Wilson and Hay 1995; Ngusaru

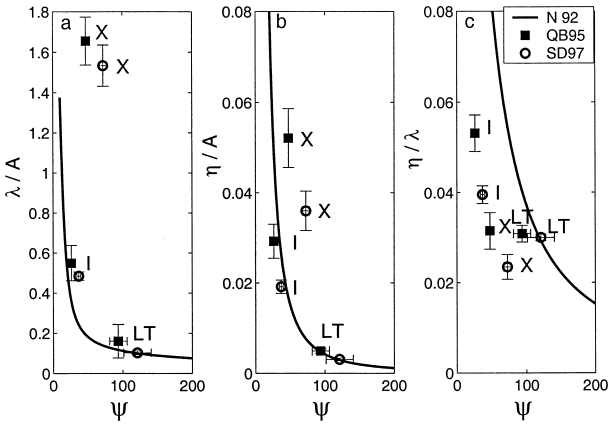

FIG. 1. Ensemble-averaged bedform dimensions for two field experiments compared with predictions by Nielsen [1992, Eqs. (3.4.3) and (3.4.8)]: (a) bedform wavelength λ, normalized by A, the significant wave semiexcursion as a function of the mobility numbers ψ; (b) normalized bedform height, η/A; and (c) bedform slope. Symbol indicators are I: irregular ripples, X: cross ripples, and LT: linear transition ripples. Error bars represent twice the standard error.

2000). The results for ripple height and wavelength are generally consistent with previous observations parameterized by Nielsen (1992, p. 137 and p. 143), except for cross ripples. In addition, the measured bed steepness for irregular and cross ripples is lower than predicted. The ripple dimensions from the two sites are similar for each of the three ripple types. However, the sediment grain size is also similar (Table 1), so it is not altogether unexpected that bed states should occur at similar wave energies at the two sites. Regression of the logarithm of the ripple heights and wavelengths shows

$$\eta = 0.029\lambda^{0.905} \tag{14}$$

with $r^2 = 0.92$. Except for one irregular ripple case, the bed steepness is nearly constant for all ripple cases, and has an approximate value of 0.03.

4. Wave friction factors, f_w

Wave friction factors were estimated using two methods. The first method provides two estimates of the friction factor and is based on the measured nearbed peak in vertical turbulence intensity, $w'_{\rm rms}$:

$$f_w = 2\left(\frac{2w'_{\rm rms}}{\tilde{u}_{\rm rms}}\right)^2, \tag{15}$$

where $\tilde{u}_{\rm rms}$ is the root-mean-square orbital velocity. In the above equation it is assumed that $w'_{\rm rms}/u_* \sim 0.5$ based on laboratory experimental evidence from van Doorn (in Nielsen 1992, p. 72), Sleath (1987), and Jensen et al. (1989), which indicate ratios between 0.5 and 0.7. Their experiments used regular waves over fixed roughness elements, and u_* was estimated from the velocity defect relation (Sleath 1987) and from log-law relations (Jensen et al. 1989). Here, vertical turbulence intensities were measured using the vertical beam of the CDP system over an O(1 m) vertical profile. Turbulent velocities were separated from wave velocities by (i) high-pass filtering the velocity time series with a 5th-order Butterworth filter with a cutoff frequency of 0.7 Hz (SD97) and 2 Hz (QB95) and (ii) using linear inviscid wave theory to remove the wave orbital velocity, thereby giving the turbulent velocity as the residual (Smyth 2001; Smyth et al. 2002).

The second method for estimating the friction factor is based on the measured horizontal velocity profile and the velocity defect relation [Eq. (4)]. This method could be applied to the QB95 data, which includes measured vertical profiles of the horizontal velocity from 3 cm to 20 cm above the bed made with a dual-beam CDP system (Zedel and Hay 1999). Thus,

$$u_*^2 = \frac{\partial}{\partial t}\int_{z_1}^{z_2} (\tilde{u}_b - \tilde{u}_{20})\, dz, \tag{16}$$

where $\tilde{u}$ is the low-pass filtered horizontal velocity (1-Hz cutoff, fifth-order Butterworth filter), the subscript 20 denotes 20 cm above the bottom, and z_2 was varied from 6 to 11 cm above the bottom. Profiles of velocity difference were estimated from $z_1 = 3$ cm to z_2 and were then extrapolated to $z_1 = 0$ using a third-order polynomial fit. These extrapolated profiles were integrated from $z = 0$ to z_2 (trapezoidal method), and then the time derivative was estimated by taking the gradient. The maximum stress was estimated for each wave, and the average stress was estimated from these maxima. A disadvantage of this procedure is that there is a wide range of estimated friction factors, but the advantage is that the results are not biased by a specific form of the velocity profile. The lower limit of the integral was taken as $z = 0$ because the value of z_0 is not well known as a function of ripple position. Assuming an approximate value of $z_0 = 4\eta/30$ has little effect on the results. In addition, the $z = 0$ position was taken as the position of the seafloor in a given data run, and was not taken with respect to a zero reference level. Thus, the stress estimates are averaged over the ripple height.

Figure 2 shows the estimated friction factors are very similar for the two methods. For each method a range of friction factors is given. The vertical turbulence intensity method, the upper limit is based on the turbulence intensity estimated from linear wave theory while the lower limit is based on the low-pass filtered estimates of the turbulence. The velocity defect method produces six estimates of the friction factor, one for each of the six different upper limits on the integration. The range of these estimates is shown in Fig. 2. Because the friction factor estimates are similar using two very different methods, it is concluded that these estimates are robust over the measured range of wave energies and bedstates.

Smyth et al. (2002) showed that these friction factors were consistent with semiempirical predictions by Tol-

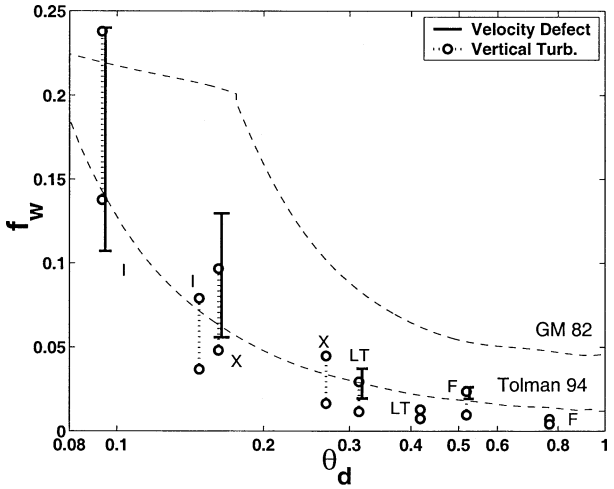

FIG. 2. Friction factors estimated using the velocity defect relation (solid vertical bars: QB95 only) and turbulence intensity (dashed vertical bars: both SD97 and QB95). Shown for comparison are the predictions from Tolman (1994) and Grant and Madsen (1982).

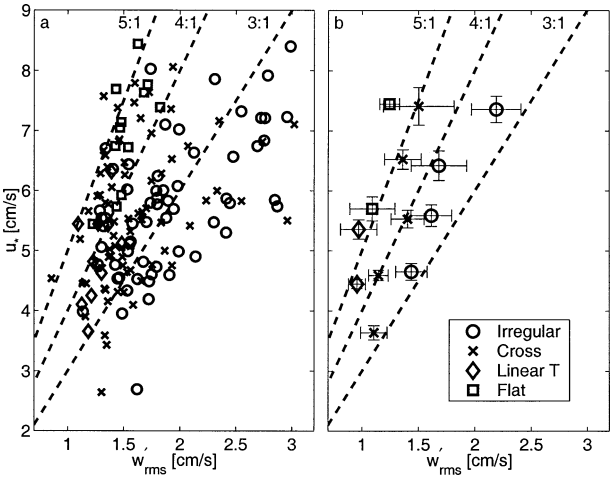

FIG. 3. Average w'_{rms} vs u_* for QB95. Values for all data runs are shown in (a) and are averaged into 1 cm s^{-1} bins using u_* values in (b). Error bars identify the standard error about the mean.

man (1994) and inconsistent with semiempirical predictions by Grant and Madsen (1982) (Fig. 2). Both of these friction factor predictions are based on a time-invariant eddy viscosity model which increases linearly with height. However, these models use different empiricisms: Grant and Madsen (1982) used laboratory estimates of bed roughness for regular waves, and Tolman (1994) used laboratory estimates of roughness for irregular waves and mobile beds, based on data from Madsen et al. (1990). Clearly their estimates of bed roughness considerably improved the model predictions. Bed roughness estimates will be examined further in the next section.

In Smyth et al. (2002) it was assumed that $u_* = 4w'_{rms}$ based on laboratory experimental evidence using regular waves and fixed roughness ($u_* = 2w'_{rms}$) and accounting for irregular wave conditions by augmenting w'_{rms} by a factor of 2. The value of this ratio may be checked for the QB95 dataset using u_* from the shear stress estimates and w'_{rms} measurements. For simplicity, w'_{rms} was taken as the average of the filter and linear wave theory methods. The values of u_* were averaged over the selected values of z_2. Figure 3 indicates that generally $u_* \sim 4w'_{rms}$, as was assumed in Smyth et al. (2002). In fact, global averages of the ratio of u_* to w'_{rms} are 3.1, 3.6, 3.9, and 4.7 for the four bed states with an ensemble average of 3.8.

In the rest of the paper, the friction factors are those estimated from the vertical turbulence intensity methods because this data is available from both datasets. Unless otherwise indicated, friction factors were ensemble-averaged over all of the data runs for each bed state to avoid bias from the larger number of low-energy data runs. Where direct comparisons are made with laboratory results, an average friction factor is estimated from the ensemble-averaged friction factor for the two velocity decomposition methods.

5. f_w versus relative roughness

Estimated friction factors are shown as a function of relative roughness, A/k_N, for all of the selected data runs from SD97 in Fig. 4. The observed scatter is comparable to that observed in laboratory measurements for regular waves over ripples and fixed roughness (Kamphuis 1975; Nielsen 1992, p. 148). The present measurements likely include additional scatter due to irregular waves and changing ripple dimensions.

Significant differences are found between the two k_N

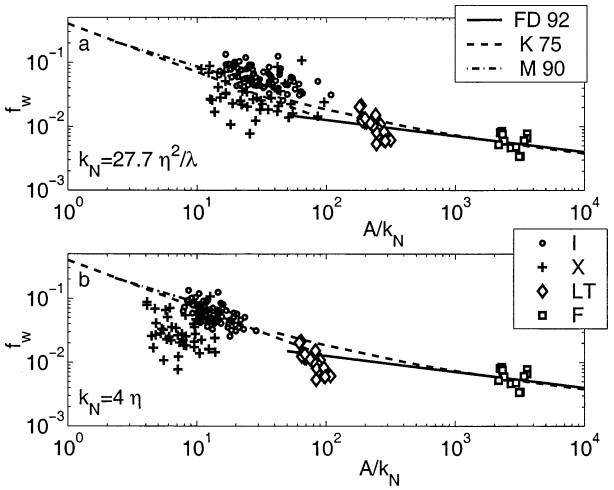

FIG. 4. Friction factors for the SD97 experiment as a function of relative roughness, A/k_N using two k_N estimators: (a) $k_N = 27.7\eta^2/\lambda$ and (b) $k_N = 4\eta$. For flat bed, $k_N = 2d_{50}$. Previous results are also shown, FD 92: Fredsoe and Deigaard (1992); K 75: Kamphuis (1975) general form and small A/k_N approximation; and M 90: Madsen et al. (1990).

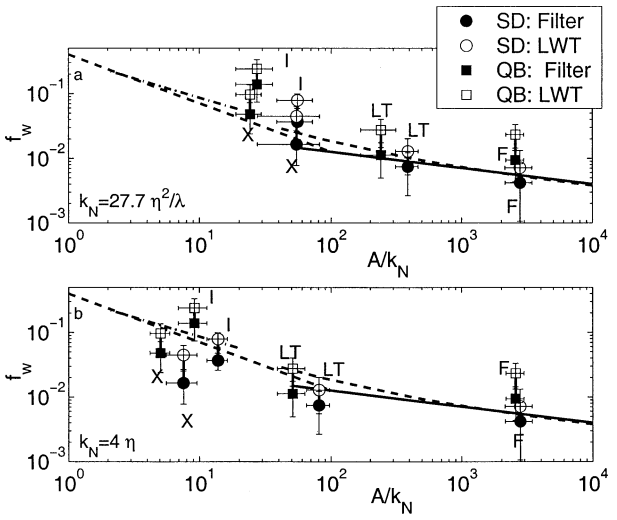

FIG. 5. Ensemble-averaged friction factors for the QB95 and SD97 experiments as a function of relative roughness, A/k_N. Symbols represent measured values for the linear wave theory method (open) and filter method (solid), a circle indicates SD97 data and a square QB95 data: (a) $k_N = 27.7\eta^2/\lambda$ and (b) $k_N = 4\eta$. For flat bed, $k_N = 2d_{50}$. Error bars are 5 times the standard error. Lines are as in Fig. 4.

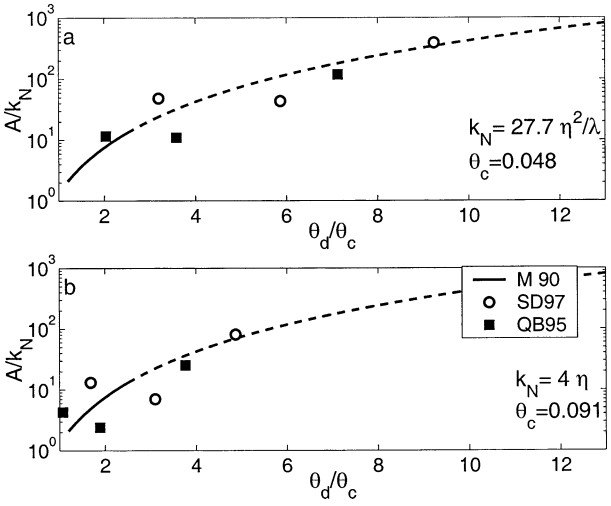

FIG. 6. Relative roughness, A/k_N, vs the normalized grain roughness Shields parameter, θ_d/θ_c. (a) Relative roughness estimated by $27.7\eta^2/\lambda$ for data from QB95 (circles) and SD97 (squares). (b) Relative roughness estimated by 4η. Also shown are the estimates from Madsen et al. (1990), originally obtained for $\theta_d/\theta_c < 3$ (solid) and extrapolated here (dashed).

parameterizations for rippled beds ($27.7\eta^2/\lambda$ and 4η), particularly for the cross ripple case. Friction factors for the high-energy cases (linear transition ripples and flat bed) are close to the theoretical result of Fredsoe and Deigaard (1992, p. 25), which, as noted in section 2, is consistent with measurements by Sleath (1987) and Jensen et al. (1989) for fixed sand roughness. This suggests that the added contribution due to moving sediment is small for this range of grain roughness Shields parameters, consistent with predictions from Wilson (1989) for nonsheet flow conditions.

Results from the QB95 experiment are consistent with results from the SD97 experiment (Fig. 5). In this figure the ensemble-averaged values are estimated as

$$\overline{f_w} = 2\left(\frac{\overline{2w'_{\rm rms}}}{\overline{\tilde{u}_{\rm rms}}}\right)^2, \tag{17}$$

where the overbar represents an ensemble-average over all realizations for a given bedstate. For both experiments, the high-energy case friction factors are close to the laboratory-based fixed roughness relations. For the lower-energy cases, the estimated friction factors show significant differences from the laboratory measurements. For $k_N = 27.7\eta^2/\lambda$ (Grant and Madsen 1982), the friction factors for cross ripples are similar to those observed by Kamphuis (1975), but friction factors for irregular ripples are not well predicted. For $k_N = 4\eta$ (Wikramanayake and Madsen 1994), the situation is reversed—friction factors for irregular ripples are better predicted than those for cross ripples. Altering the expressions for the bed roughness by changing the constant (27.7 or 4) does not significantly affect the results.

The laboratory measurements of the wave friction factors over mobile beds and irregular waves by Madsen et al. (1990) are the closest set of measurements for comparison, but span a small range of wave energies. It is of interest to extrapolate their results to higher wave energies and compare them to the present measurements. Figure 6 shows measured values of A/k_N for the two k_N estimates and Eq. (12) extrapolated to higher grain roughness Shields parameters. Regression correlation coefficients for measured and predicted values are similar for the two cases: $r^2 = 0.9$ for $k_N = 27.7\eta^2/\lambda$ as compared with $r^2 = 0.87$ for $k_N = 4\eta$. The critical Shields parameter was selected as the value that gave the best fit between the measured and extrapolated k_N. For $k_N = 27\eta^2/\lambda$, the critical Shields parameter was 0.048, consistent with previous measurements of $\theta_c \sim 0.05$ (Nielsen 1992, p. 107). For $k_N = 4\eta$, θ_c was found to be 0.091, much higher than the expected value. This result suggests that $k_N = 27.7(\eta^2/\lambda)$ is the better parameterization of the two, and therefore that ripple steepness contributes importantly to the effective roughness.

6. The f_w variation with Reynolds number

Jonsson (1966) proposed an f_w versus Re diagram equivalent to the Stanton diagram for pipe flow. The Reynolds number is defined as

$$\mathrm{Re} = \frac{\tilde{u}_{1/3}A}{\nu}, \tag{18}$$

where $\tilde{u}_{1/3}$ is the significant wave orbital velocity, A is the semiexcursion based on $\tilde{u}_{1/3}$, and ν is the fluid kinematic viscosity.

Several studies have helped to define the various re-

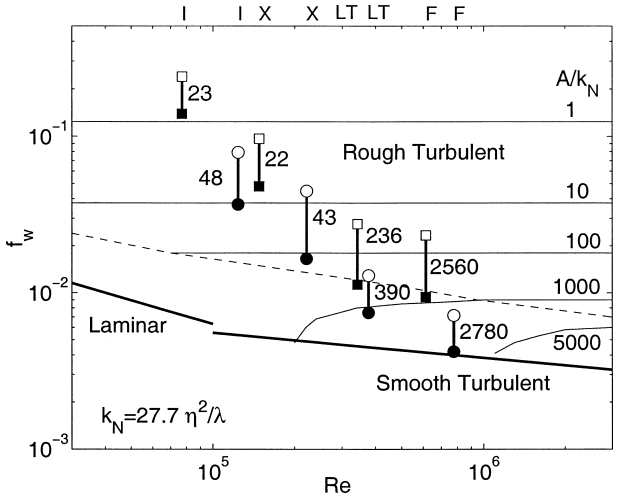

FIG. 7. Ensemble-average friction factors for two experiments as a function of Reynolds number. Open symbols indicate friction factors estimated from the linear wave theory method; closed symbols: filter method; circles: SD97; squares: QB95 data. Numbers beside the measurements indicate the value of A/k_N. Also indicated are the laminar regime, smooth-turbulent regime (Fredsoe and Deigaard 1992), and rough-turbulent and (dashed line) transition region for a variety of A/k_N values [approximate A/k_N values from Fig. 5.47 in Justesen (1988)].

gions of Jonsson's early diagram. As indicated in Fig. 7, there is a low Reynolds number laminar regime, a high Reynolds number smooth-turbulent regime and a rough-turbulent regime partitioned by A/k_N values. Theoretical work by Fredsoe and Deigaard (1992) defined the smooth-turbulent curve which agrees well with laboratory measurements by Jensen et al. (1989) with fixed roughness and regular waves. The rough-turbulent A/k_N lines were obtained by Justesen (1988) using a turbulent kinetic energy model and are generally consistent with laboratory measurements made by Kamphuis (1975) over fixed grain roughness using regular waves. There was, however, considerable scatter in the laboratory measurements.

The field measurements also exhibit a large range of friction factors for a given Reynolds number (Fig. 7), but generally occupy a fairly narrow band in this parameter space. A log–log fit of the ensemble-averaged friction factors versus Reynolds number gives

$$\log \overline{f_w} = -1.34 \log \overline{\mathrm{Re}} + 13.1, \qquad (19)$$

with $r^2 = 0.9$. Low energy ripples are in the rough turbulent regime with low Reynolds numbers and low relative roughness. High energy ripples and flat bed are in the transitional region, between smooth and rough turbulent regimes. Even though there is a considerable range of friction factors due to the two turbulence intensity estimates, the measurements are not always consistent with the A/k_N lines predicted by Justesen (1988). This result may in part be due to the inability of the model to predict turbulence intensities caused by vortex shedding, but may also be due to the selected parameterization of the bed roughness ($k_N = 27.7\eta^2/\lambda$).

TABLE 2. Linear regression slopes and squared regression correlation coefficient r^2 for potential f_w variables.

Ordinate	Abscissa	Slope	r^2
$\log(A/\eta)$	$\log(A/\lambda)$	−0.97	0.94
$\log(\lambda/\eta)$	$\log(A/\lambda)$	−0.026	0.01
$\log A$	$\log \eta$	−0.19	0.34
$\log A$	$\log \lambda$	−0.11	0.12
$\log \eta$	$\log \lambda$	0.9	0.92

7. Roughness formulation

The parameterization of bed roughness is investigated through regression of measured friction factors, wave semiexcursion distances and ripple dimensions. It is assumed that the friction factor is a function of three nondimensional variables: A/η, A/λ, and λ/η. These variables were regressed against each other to check for colinearities (Table 2). Because $\log(A/\eta)$ and $\log(A/\lambda)$ are highly correlated, only one of these variable pairs may be used.

Stepwise regression of $\log(\overline{f_w})$ with $\log(A/\eta)$ and $\log(\lambda/\eta)$ shows that both terms are important (Table 3). Also in this table are the coefficients α and β, where

$$\log(f_w) = \alpha \log(A/\eta) + \beta \log(\lambda/\eta) + \gamma \qquad (20)$$

and γ is a constant equal to 7.34 from the fit. Rearranging this expression by choosing the form

$$f_w = c_1 \left(\frac{A}{k_N}\right)^{\alpha} \qquad (21)$$

gives

$$k_N = c_2 \left(\frac{\eta}{\lambda}\right)^{\beta/\alpha} \eta, \qquad (22)$$

where $\alpha = -0.623$, $\beta = -2.337$, c_1 and c_2 are constants and are related by $c_2 = (c_1/\delta)^{1/\alpha}$ where $\gamma = \log\delta$. The roughness constant c_2 was obtained by minimizing the square error between friction factors predicted from Eq. (21) and those predicted from roughness estimates by Kamphuis (1975) for $A/k_N < 80$ [Eq. (9)], and by Fredsoe and Deigaard (1992) for $A/k_N > 80$ [Eq. (6)]. Substituting in the coefficients gives

TABLE 3. The f_w regression slopes, 95% confidence intervals (in brackets), and associated r^2 and p values.

Term(s)	Slope	r^2	p
$\log(A/\eta)$	−0.71 (0.80)	0.60	0.07
$\log(\lambda/\eta)$	−2.7 (3.6)	0.52	0.10
$\log(A/\eta)$, $\log(\lambda/\eta)$	−0.63 (0.21), −2.3 (0.9)	0.98	0.002

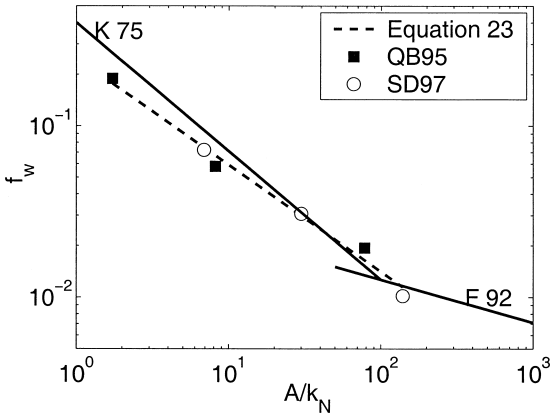

FIG. 8. Friction factors based on Eq. (23a), along with measurements. Also indicated are the smooth-turbulent regime from Fredsoe and Deigaard (1992) and the small A/k_N approximation from Kamphuis (1975).

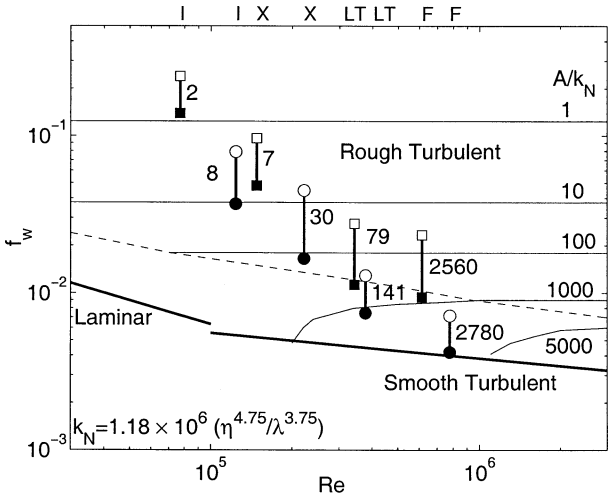

FIG. 9. As in Fig. 7 but with new estimates of k_N based on Eq. (23b).

$$f_w = 0.247\left(\frac{A}{k_N}\right)^{-0.623} \tag{23a}$$

$$k_N = 1.18 \times 10^6\left(\frac{\eta}{\lambda}\right)^{3.75}\eta. \tag{23b}$$

Based on the 95% confidence intervals, the value of β/α has a range of 1.90–7.23, and more data are required to more accurately estimate the ripple steepness exponent. However, this new roughness parameterization suggests a much stronger dependence on ripple steepness than the linear dependence predicted by Grant and Madsen (1982).

Figure 8 shows that, with the new formulation of k_N, the data points lie almost on a straight line. It is interesting to note that substituting an approximate ripple steepness of 0.03 in the above expression gives $k_N = 2.3\eta$, a similar result to Wikramanayake and Madsen (1994). Using the new estimates of bed roughness from Eq. (23b), predicted A/k_N values agree more closely with predictions from Justesen (1988), as shown in Fig. 9.

Ensemble-average friction factors regressed with the semiorbital excursion have a strong correlation ($r^2 = 0.85$), and suggests a simpler form of the friction factor will provide reasonably good predictions. The slope of $\log(f_w)$ versus $\log(A/d_{50})$ ranges from -2.25 to -2.78 (Fig. 10). High correlation coefficients are partially explained by the fact that f_w is controlled by the inverse square of the wave velocity as the shear velocity is nearly constant for the four bed states [Eq. (1)]. It is interesting that this expression for f_w is similar to the laboratory results of Madsen et al. (1990) [Eq. (12)], where the friction factor is given in terms of the grain roughness Shields parameter raised to the power -1.5, which approximately gives $\log(f_w) = -3A/d$. Additional data are needed to more precisely determine the value of the slope.

8. Conclusions

Wave friction factors estimated from field measurements of wave velocity, bedform geometry, and near-bed turbulent velocities have been examined as a function of relative roughness and Reynolds number. Results have been compared to previous empirical laboratory results, model predictions, and theoretical results.

Friction factors estimated from the integrated acceleration defect equation, as well as from u_* estimates using vertical turbulence intensity measurements, give similar results.

As a function of relative roughness, friction factor estimates are found to agree with results by Kamphuis (1975) when bed roughness is based on ripple height and wavelength (Grant and Madsen 1982), although

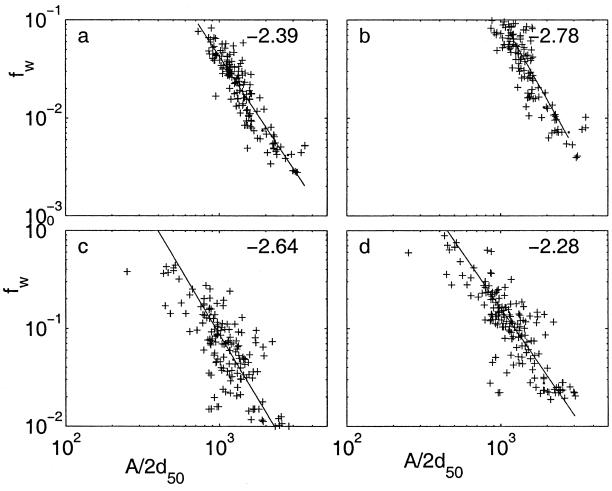

FIG. 10. Measured friction factors as a function of $A/2d_{50}$; SD97 results are shown for (a) the filter method and for (b) the linear wave theory method. Corresponding QB95 results are shown in (c) and (d).

there are some discrepancies. There is also good agreement between relative roughness estimates and extrapolated results from Madsen et al. (1990), which suggests that their roughness estimate [Eq. (12)] is valid over a wider range of wave energies. A new expression for the bed roughness was derived through regression analysis of measured friction factors and three length scales: A, η, and λ. A reasonably good predictor of f_w for all bed states appears to be $f_w \sim A^{-2.5}$. Selecting the traditional form of f_w versus A/k_N and regressing f_w with two nondimensional groups, A/λ and η/λ, gives a new expression for the bed roughness: $k_N \sim (\eta/\lambda)^{3.75}\eta$. This expression indicates a higher sensitivity of k_N to ripple steepness as compared with steady-flow results where $k_N \sim (\eta/\lambda)\eta$ (Grant and Madsen 1982).

Measured friction factors for the high-energy cases approach fixed roughness values, which suggests the moving grain roughness contribution is small. This observation is consistent with predictions by Wilson (1989) for the range of grain roughness Shields parameters encompassed in this study.

As a function of Reynolds number, measured friction factors agree reasonably well with model predictions by Justesen (1988) and laboratory results by Kamphuis (1975). The field measurements occupy a relatively narrow band on the f_w–Re diagram and exhibit a power-law dependence. Low-energy conditions fall in the rough turbulent regime and high-energy conditions are in the transition zone between smooth and rough turbulent regimes.

Acknowledgments. This work was funded by the U.S. Office of Naval Research, Coastal Sciences Program, and the Natural Sciences and Engineering Research Council of Canada.

REFERENCES

Ardhuin, F., T. H. C. Herbers, and W. C. O'Reilly, 2001: A hybrid Eulerian–Lagrangian model for spectral wave evolution with applications to bottom friction on the continental shelf. *J. Phys. Oceanogr.,* **31,** 498–1516.

Crawford, A. M., and A. E. Hay, 2001: Linear transition ripple migration and wave orbital velocity skewness: Observations. *J. Geophys. Res.,* **106,** 14 113–14 128.

Fredsoe, J., and R. Deigaard, 1992: *Mechanics of Coastal Sediment Transport.* World Scientific, 369 pp.

Grant, W. D., and O. S. Madsen, 1982: Movable bed roughness in unsteady oscillatory flow. *J. Geophys. Res.,* **87,** 469–481.

Hay, A. E., and D. J. Wilson, 1994: Rotary sidescan images of nearshore bedform evolution during a storm. *Mar. Geol.,* **119,** 57–67.

Jensen, B. L., B. M. Sumer, and J. Fredsoe, 1989: Turbulent oscillatory boundary layers at high Reynolds numbers. *J. Fluid Mech.,* **206,** 265–297.

Jonsson, I. G., 1966: Wave boundary layers and friction factors. *Proc. 10th Int. Conf. on Coastal Engineering,* Tokyo, Japan, ASCE, 127–148.

Justesen, P., 1988: Turbulent wave boundary layers. Ph.D. thesis, Technical University of Denmark, 226 pp.

Kamphuis, J. W., 1975: Friction factor under oscillatory waves. *J. Waterw. Harbor Coastal Eng. Div.,* **101,** 135–145.

Madsen, O. S., Y. Poon, and H. C. Graber, 1988: Spectral wave attenuation by bottom friction: Theory. *Proc. 21st Int. Conf. on Coastal Engineering,* Delft, Netherlands, ASCE, 492–503.

——, P. P. Mathiesen, and M. M. Rosengaus, 1990: Movable bed friction factors for spectral waves. *Proc. 22d Int. Conf. on Coastal Engineering,* Delft, Netherlands, ASCE, 420–429.

Ngusaru, A. S., 2000: Cross-shore migration of lunate mega-ripples and bedload sediment transport models. Ph.D. thesis, Memorial University, 193 pp.

Nielsen, P., 1992: *Coastal Bottom Boundary Layers and Sediment Transport.* World Scientific, 324 pp.

Sleath, J. F. A., 1987: Turbulent oscillatory flow over rough beds. *J. Fluid Mech.,* **182,** 369–409.

——, 1995: Sediment transport by waves and currents. *J. Geophys. Res.,* **100** (C6), 10 977–10 986.

Smyth, C., 2001: Coherent Doppler profiler measurements of near-bed vertical suspended sediment fluxes for different bedstates in the nearshore zone. Ph.D. thesis, Dalhousie University, 152 pp.

——, A. E. Hay, and L. Zedel, 2002: Coherent Doppler profiler measurements of near-bed suspended sediment fluxes and the influence of bedforms. *J. Geophys. Res.,* in press.

Tolman, H. L., 1994: Wind waves and movable-bed bottom friction. *J. Phys. Oceanogr.,* **24,** 994–1009.

Vincent, C. E., D. M. Hanes, and A. J. Bowen, 1991: Acoustic measurements of suspended sand on the shoreface and the control of concentration by bed roughness. *Mar. Geol.,* **91,** 1–18.

Wikramanayake, P. N., and O. S. Madsen, 1994: Calculation of movable bed friction factors. Tech. Rep. DRP-94-5, U.S. Army Corps of Engineers, Coastal Engineering Research Center, Vicksburg, MS, 104 pp.

Wilson, D. J., and A. E. Hay, 1995: High resolution sidescan sonar observations of small scale sand bedforms under waves: A comparison of field and laboratory measurements. *Proc. 1995 Canadian Coastal Conf.,* Ottawa, ON, Canada, Canadian Coastal Science and Engineering Association.

Wilson, K. C., 1989: Friction of wave-induced sheet flow. *Coastal Eng.,* **12,** 371–379.

Young, I. R., and R. M. Gorman, 1995: Measurements of the evolution of ocean wave spectra due to bottom friction. *J. Geophys. Res.,* **100,** 10 987–11 004.

Zedel, L., and A. E. Hay, 1999: A Coherent Doppler profiler for high resolution particle velocimetry in the ocean: Laboratory measurements of turbulence and particle flux. *J. Atmos. Oceanic Technol.,* **16,** 1102–1117.